Wang, Xiyu; Yiğitler, Hüseyin; Jäntti, Riku

Gaining from Multiple Ambient Sources: Signaling Matrix for Multi-Antenna Backscatter Devices

Published in:
IEEE Wireless Communications Letters

DOI:
10.1109/LWC.2022.3231907

Published: 01/01/2022

Document Version
Publisher's PDF, also known as Version of record

Gaining From Multiple Ambient Sources: Signaling Matrix for Multi-Antenna Backscatter Devices

Xiyu Wang, *Graduate Student Member, IEEE*, Hüseyin Yiğitler, and Riku Jäntti, *Senior Member, IEEE*

***Abstract*—The backscatter device (BD) in ambient backscatter communication (AmBC) systems is often illuminated by multiple ambient sources in reality. Although multiple ambient sources can benefit the AmBC systems, this scenario has been rarely studied. This letter gives an answer to the overlooked question of how to effectively obtain the gain from multiple ambient sources—using a proper signaling matrix on a multi-antenna BD. We optimize the BD signaling matrix based on the criterion of minimizing the AmBC system bit-error-rate (BER) performance. The derived signaling matrices combine the ambient signals and steer the backscatter signal toward the receiver to increase the received signal strength. The simulation results show that the multi-antenna BD effectively uses multiple ambient sources, and the derived BD signaling matrices robustly achieve a larger communication range or a higher datarate of AmBC systems.**

***Index Terms*—Ambient backscatter communications, multiple antennas, signaling matrix, performance analysis.**

I. Introduction

AMBIENT backscatter communication (AmBC) is a promising paradigm for realizing sustainable Internet-of-Things (IoT) [1]. The limited system performance caused by the low signal-to-interference-plus-noise ratio (SINR) of the desired signal hinders it from a wider acceptance. Although many efforts have been devoted into the multi-antenna AmBC receiver designs [2], [3], [4], [5], [6], these works consider a single ambient source such that a more practical scenario where signals that come from multiple ambient sources impinging on BD is overlooked. Multiple ambient sources potentially benefit the AmBC systems by providing higher signal power that can be harvested and backscattered, which boosts the signal-to-noise ratio (SNR) of the target signal. With that being said, multiple ambient sources are not effectively exploited.

Effective use of multiple ambient sources is challenging since more sources add more unknown parameters. In a wideband AmBC system [7], the receiver demodulates the BD signal by looking into the frequency band of individual ambient sources and then, using the maximal ratio combining to combine extracted backscatter signal together. This system requires an ultra wideband receiver. An alternative way of tackling this challenge is to use a multi-antenna BD. In principle, the BD tunes its reflection coefficients, which is referred to as *signaling matrix*, to steer the signal towards the strongest backscatter signal direction. The work [8] demonstrates the concept that finding a proper angle for the BD array can maximize the backscatter signal experimentally. However, BD signaling matrix is not further investigated.

Recently, multi-antennas BDs are proposed to improve the system performance using different transmission schemes. For instance, the BD may wake up the best antenna [9] or a group of antennas [10] to obtain a diversity gain. The work [11] realizes orthogonal space-time coding at BD. The work [12] presents a printed BD array that achieves gigabit datarate communication in a mono-static scenario. However, these works have not considered multiple ambient sources. Furthermore, these BDs do not allow signal transfer between antenna elements. This corresponds to either the *identity signaling matrix* if the signals transmitted from antennas are the same, or the *diagonal signaling matrix* [13]. The *full signaling matrix* that potentially provides additional gains and degrees-of-freedom is little-studied.

In this letter, we study the problem of using a multi-antenna BD to fully exploit multiple ambient sources. We investigate the optimum full and diagonal BD signaling matrices that improve the AmBC system performance. Our approach finds the strongest signal directions transmitted from multiple ambient sources and backscattered toward the receiver.

The contributions of the work are summarized as follows:

- We define an optimization problem that yields the BD signaling matrix minimizing the AmBC bit-error-rate (BER) performance, which is intractable due to the innate property of AmBC systems. Thus, we propose a relaxation. The obtained optimum full BD signaling matrix is a beamforming matrix that steers the backscatter signal in the direction of the strongest signal strength. For a simpler implementation, we also derive the optimum diagonal BD signaling matrix.
- We provide a BD modulator diagram for transmitting the full signaling matrix. We propose a practical estimation approach for implementing the optimum BD signaling matrices.
- We evaluate the BD signaling matrices in terms of BER using an AmBC receiver extended from a previous work. The simulation results demonstrate that using a multi-antenna BD is necessary for effectively using multiple ambient sources. The derived BD signaling matrices provide a robust improvement to the BER performance. It is also shown that the optimum full signaling matrix obtains a performance gain compared with the diagonal one at the cost of higher implementation complexity.

Notations: Complex scalars are assumed, and their set is denoted by $\mathbb{C}$. The $n \times n$ identity matrix is $\boldsymbol{I}_n$, and the subscript n may be omitted occasionally for simplicity. The circularly symmetric complex Gaussian distribution with mean $\boldsymbol{a}$ and covariance matrix $\boldsymbol{A}$ is $\mathcal{CN}(\boldsymbol{a}, \boldsymbol{A})$. For vector $\boldsymbol{a}$, the Euclidean norm is $\|\boldsymbol{a}\|$, the infinity norm is $\|\boldsymbol{a}\|_\infty$. The square diagonal matrix with entries $\boldsymbol{a}$ is $\mathrm{diag}(\boldsymbol{a})$. For matrix $\boldsymbol{A}$, the Frobenius norm is $|||\boldsymbol{A}|||_F$, the spectral norm is $|||\boldsymbol{A}|||_2$. The

Manuscript received 12 November 2022; accepted 15 December 2022. Date of publication 26 December 2022; date of current version 9 March 2023. This work was supported in part by the Academy of Finland BESIMAL Project under Grant 334197. The associate editor coordinating the review of this article and approving it for publication was X. Lei. *(Corresponding author: Xiyu Wang.)*

The authors are with the Department of Communications and Networking, Aalto University, 02150 Espoo, Finland (e-mail: xiyu.wang@aalto.fi; huseyin.yigitler@aalto.fi; riku.jantti@aalto.fi).

Digital Object Identifier 10.1109/LWC.2022.3231907

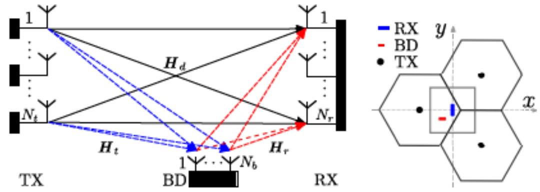

(a) (b)

Fig. 1. In (a), an illustration of a bistatic multi-antenna AmBC system. In (b), a practical scenario where the grey square marks the selected area for Section V.

conjugate-transpose, conjugate, and transpose are A^H, A^*, and A^T, and its determinant is $|A|$. The vectorization, and the matricization are given by $\mathrm{vec}(A)$ and $\mathrm{vec}^{-1}(A)$. $\mathrm{diag}(A)$ returns the vector of the diagonal entries. The i-th column vector of A is $[A]_i$. The i-th row and the j-th column entry is $[A]_{i,j}$. The Hadamard and Kronecker products of matrices are denoted by symbols $\circ$ and $\otimes$.

II. System Model

A typical bistatic AmBC system is considered as shown in Fig. 1(a), where the BD has N_b antennas, the receiver (RX) has N_r antennas, and there are N_t single-antenna transmitters (TX) from legacy systems. A practical scenario is illustrated in Fig. 1(b). The BD and the RX are assumed to be equipped with a uniform linear array with half-wavelength, i.e., $\lambda/2$, separation between two antenna elements.

We consider a *quasi-static* deployment where the system components move sufficiently slow so that the channels can be safely assumed constant for the time duration of interest. Let $\tilde{H}_d \in \mathbb{C}^{N_r \times N_t}$, $\tilde{H}_r \in \mathbb{C}^{N_r \times N_b}$, and $\tilde{H}_t \in \mathbb{C}^{N_b \times N_t}$ be the large-scale spatial average of TX-RX, BD-RX and TX-BD, respectively, which are in general defined by the geometry and free-space path loss. The received signal at the RX array is a superposition of the direct path signal and the backscatter signal. The k-th sample of noise-free received signal is

$$\tilde{y}[k] = \tilde{H}_d s[k] + \sqrt{\alpha}\tilde{H}_r X[k]\tilde{H}_t s[k],$$

where α is the BD modulator circuit implementation loss [5], s is the ambient signal transmitted from TXs, X denotes the BD signal which is referred to as the *BD signaling matrix*.

In order to represent the SNR in terms of transmit power of the ambient sources while keeping the power difference between two paths, the channel matrices are normalized with respect to $\tilde{H}_d$, i.e.,

$$H_d = \tilde{H}_d / \left(\left\| \tilde{H}_d \right\|_F / \sqrt{N_r N_t} \right)$$

such that $\|H_d\|_F^2 = N_r N_t$. Then, the received signal is given by

$$y[k] = H_d s[k] + \sqrt{\Delta} H_r X[k] H_t s[k] + n[k] \qquad (1)$$

where $n \sim \mathcal{CN}(\mathbf{0}, I)$ denotes additive white Gaussian noise at the RX whose components are independent of the components of s and X, channel matrices H_r and H_t are normalized such that $\|H_r\|_F^2 = N_r N_b$, $s\|H_t\|_F^2 = N_b N_t$, and

$$\Delta = \alpha \left\| \tilde{H}_r \right\|_F^2 \left\| \tilde{H}_t \right\|_F^2 / \left(\left\| \tilde{H}_d \right\|_F^2 N_b^2 \right)$$

is the ratio of the backscatter signal power to the ambient signal power. Then, the SNR of the direct path signal per TX per RX antenna is defined as $\gamma = P_s$.

Considering that the multiple ambient sources transmit their signal individually, the elements of s are different and have a high variation in amplitudes. Hence, we assume that the elements of s are independent identical distributed (i.i.d.) *Gaussian* variables with the same average transmit power P_s, i.e., $s \sim \mathcal{CN}(\mathbf{0}, P_s I)$. It is a close approximation to realistic radio frequency signals with complex modulations, such as the OFDM sources.

In what follows, the time dependence of y is dropped since the analysis is restrict to the single temporal sample. We assume that the BD and the RX are perfectly synchronized.[1] Then, Eq. (1) can be rewritten as

$$y = G(X)s + n, \;\; G(X) = H_d + \sqrt{\Delta} H_r X H_t, \qquad (2)$$

where we denote $G(X)$ as the *composite channel matrix*.

III. The Optimum BD Signaling Matrix

BD signaling matrix, denoted by $X \in \mathbb{C}^{N_b \times N_b}$, represents the reflection coefficients on the N_b BD antennas. Three forms of signaling matrix depending on the physical implementation of the modulation circuitry are described in [13]. It is worth noting that, first, there is no power amplification on the passive BD such that the BD signaling matrix has a power constraint

$$0 \leq \|[X]_j\|^2 \leq 1, j = 1, \ldots, N_b. \qquad (3)$$

It arises from the fact that the incident signal power on a single BD antenna element will not be amplified after modulation. Second, the BD signal can assume two equiprobable values, i.e., $X \in \{X_0, X_1\}$ is binary-modulated and $p(X_0) = p(X_1) = 0.5$.

For deriving the optimum BD signaling matrix, let us first assume that the ambient signal and the channel matrices are known. In this case, $y \sim \mathcal{CN}(G(X)s, I)$. Applying the maximum-a-posteriori (MAP) criterion and taking logarithm on both sides, the binary hypotheses testing is [14, Ch. 4]

$$\begin{aligned} z \triangleq\; & \mathrm{Re}\{y^H H_r (X_0 - X_1) H_t s\} \\ \underset{\mathcal{H}_1}{\overset{\mathcal{H}_0}{\gtrless}}\; & \mathrm{Re}\{s^H H_d^H H_r (X_0 - X_1) H_t s\} \\ & + \sqrt{\Delta}\Big(\|H_r X_0 H_t s\|^2 - \|H_r X_1 H_t s\|^2 \Big)/2. \end{aligned}$$

The test statistic z is a Gaussian random variable with mean $\mathrm{Re}\{s^H H_t^H (X_0 - X_1)^H H_r^H G(X)s\}$ and variance $\|H_r(X_0 - X_1)H_t s\|^2/2$. Thus, the error probability is $p_e = \mathcal{Q}(\sqrt{\Delta/2}\|H_r(X_0 - X_1)H_t s\|)$, where $\mathcal{Q}(\cdot)$ denotes the Q-function [15, Ch. 3]. Since the Q-function is monotonic decreasing, the error probability p_e is minimized by maximizing the L2-norm $\|H_r(X_0 - X_1)H_t s\|$ which indicates the distance between the two states of backscattered path signal. Then, the problem of minimizing p_e can be equivalently written as

$$\begin{aligned} \underset{X_0, X_1}{\text{maximize}} \;\; & \|H_r(X_0 - X_1)H_t s\|^2 \\ \text{subject to} \;\; & 0 \leq \|[X_i]_j\|^2 \leq 1, \;\; i = 0, 1, \;\; j = 1, \ldots, N_b. \end{aligned} \qquad (4)$$

Remark 1: The global optima of problem (4) depends on the ambient signal s. When s is known, the optimum $X_0 -$

[1] The AmBC system does not specifically require its synchronization with the legacy system. However, it requires the presence of the ambient signal.

$\boldsymbol{X}_1$ is chosen so that s is the eigenvector associated with the largest eigenvalue of matrix $\boldsymbol{H}_r(\boldsymbol{X}_0 - \boldsymbol{X}_1)\boldsymbol{H}_t$. However, this requirement is challenging for two reasons. One is that the AmBC receiver is agnostic about the ambient signal s due to the independence between the legacy system and the AmBC system. The other is that it is unlikely to find the optimal solution for $\boldsymbol{X}$ which changes with every realization of the fast-varying s. Hence, one needs to apply a relaxation to solve the original problem.

The objective function of problem (4) satisfies the inequality

$$\begin{aligned}\|\boldsymbol{H}_r(\boldsymbol{X}_0 - \boldsymbol{X}_1)\boldsymbol{H}_t s\|^2 &\le |||\boldsymbol{H}_r(\boldsymbol{X}_0 - \boldsymbol{X}_1)\boldsymbol{H}_t|||_2^2\|s\|^2 \\ &\le |||\boldsymbol{H}_r(\boldsymbol{X}_0 - \boldsymbol{X}_1)\boldsymbol{H}_t|||_F^2\|s\|^2.\end{aligned}$$

Since $\|s\|^2$ is the total transmit power from N_t ambient sources, which is a deterministic scalar and independent of $\boldsymbol{X}_i$, the objective function can be heuristically relaxed to its upper bound, i.e., the Frobenius norm. Similarly, the constraint can be also relaxed to $|||\boldsymbol{X}|||_F^2 = \sum_{j=1}^{N_b} \|[\boldsymbol{X}]_j\|^2 \le N_b$. As a result, the relaxed optimization is given by

$$\begin{aligned}&\underset{\boldsymbol{X}_0,\boldsymbol{X}_1}{\text{maximize}} \quad |||\boldsymbol{H}_r(\boldsymbol{X}_0 - \boldsymbol{X}_1)\boldsymbol{H}_t|||_F^2 \\ &\text{subject to} \quad 0 \le |||\boldsymbol{X}_i|||_F^2 \le N_b, i = 0, 1\end{aligned} \tag{5}$$

It is worth noting that the relaxed objective function is equal to the square of the expected distance between two states of backscatter signal that averages over the i.i.d. s, that is

$$|||\boldsymbol{H}_r(\boldsymbol{X}_0 - \boldsymbol{X}_1)\boldsymbol{H}_t|||_F^2 = \mathrm{E}_s\{\|\boldsymbol{H}_r(\boldsymbol{X}_0 - \boldsymbol{X}_1)\boldsymbol{H}_t s\|^2\},$$

where E_s denotes averaging over the space of s. Hence, the relaxed function extricates minimizing p_e from relying on temporal samples of s, but in an expected sense.

A. Full BD Signaling Matrix

Let us represent the Frobenius norm in problem (5) in terms of Kronecker product and matrix vectorization as

$$|||\boldsymbol{H}_r(\boldsymbol{X}_0 - \boldsymbol{X}_1)\boldsymbol{H}_t|||_F^2 = \mathrm{vec}(\boldsymbol{X}_0 - \boldsymbol{X}_1)^H \mathbf{H}^{(1)} \mathrm{vec}(\boldsymbol{X}_0 - \boldsymbol{X}_1).$$

where we denote $\boldsymbol{Q} = \boldsymbol{H}_t^T \otimes \boldsymbol{H}_r$ and

$$\mathbf{H}^{(1)} = (\boldsymbol{H}_t\boldsymbol{H}_t^H)^T \otimes (\boldsymbol{H}_r^H\boldsymbol{H}_r) = \boldsymbol{Q}^H\boldsymbol{Q}. \tag{6}$$

Proposition 1: The optimum full signaling matrix is

$$\boldsymbol{X}_0 = -\boldsymbol{X}_1 = \boldsymbol{X}^\star = (1/\|[\boldsymbol{U}_t]_1\|_\infty)[\boldsymbol{V}_r]_1[\boldsymbol{U}_t]_1^H, \tag{7}$$

and the composite channel matrix in this case is given by

$$\boldsymbol{G}(\boldsymbol{X}_i) = \boldsymbol{H}_d + (-1)^i(\sqrt{\Delta}\sigma_{r,1}\sigma_{t,1}/\|[\boldsymbol{U}_t]_1\|_\infty)[\boldsymbol{U}_r]_1[\boldsymbol{V}_t]_1^H,$$

where $1/\|[\boldsymbol{U}_t]_1\|_\infty$ is multiplied to satisfy the power constraint in Eq. (3). $[\boldsymbol{U}_m]_1$ and $[\boldsymbol{V}_m]_1$ denote, respectively, the left- and the right-singular vector of $\boldsymbol{H}_m, m \in \{r, t\}$ associated with the largest singular value denoted by $\sigma_{m,1}$.

Proof: We use the Karush-Kuhn-Tucker (KKT) conditions by introducing two Lagrange multipliers μ_1 and μ_2 to solve the relaxed problem. Then, the KKT conditions imply:

1) $\mu_1 = \mu_2 = 0$, we have $\mathbf{H}^{(1)}\mathrm{vec}(\boldsymbol{X}_0 - \boldsymbol{X}_1) = 0$, which implies that $\mathrm{vec}(\boldsymbol{X}_0 - \boldsymbol{X}_1)$ is in the null space of $\mathbf{H}^{(1)}$.
2) $|||\boldsymbol{X}_0|||_F^2 = |||\boldsymbol{X}_1|||_F^2 = N_b$ and $\mu_1 = \mu_2 > 0$, we have that $\mathrm{vec}(\boldsymbol{X}_0) = -\mathrm{vec}(\boldsymbol{X}_1)$ are eigenvectors of matrix $\mathbf{H}^{(1)}$.

The two cases require the eigenvectors of $\mathbf{H}^{(1)}$. For that, we invoke a known theorem in matrix analysis, which states that, when $\boldsymbol{A}$ and $\boldsymbol{B}$ are diagonalizable, the eigendecomposition of $\boldsymbol{A} \otimes \boldsymbol{B}$ is formed by all the eigenvectors and the corresponding eigenvalues of $\boldsymbol{A}$ and $\boldsymbol{B}$ (see, e.g., [16, Th. 4.2.12]). Then, let the singular value decomposition (SVD) of $\boldsymbol{H}_m, m \in \{r, t\}$ be $\boldsymbol{H}_m = \boldsymbol{U}_m\boldsymbol{S}_m\boldsymbol{V}_m^H$, where the columns of unitary matrices $\boldsymbol{U}_m$ and $\boldsymbol{V}_m$ are the left- and right-singular vectors, respectively, and rectangular diagonal matrix $\boldsymbol{S}_m$ consists descending-ordered singular values whose i-th value is $\sigma_{m,i}$. Hence, $[\boldsymbol{U}_t]_i^* \otimes [\boldsymbol{V}_r]_j$ are the eigenvectors of $\mathbf{H}^{(1)}$ associated with eigenvalues $\sigma_{r,i}^2\sigma_{t,j}^2, \forall i, j = 1, \ldots, N_b$.

By comparing the values of the objective function at the local optima between two cases, the optimal solution of problem (5) is found as in case 2). In addition, the original constraint is convex. Hence, the optimum can be found at an extreme of the original feasible set which is given by Eq. (7). ■

The solution in Eq. (7) is also feasible for the induced L2-norm $|||\boldsymbol{H}_r(\boldsymbol{X}_0 - \boldsymbol{X}_1)\boldsymbol{H}_t|||_2^2$, and thus, it is closer to the optimum solution of the original problem.

When there is one ambient source, i.e., $N_t = 1$, the solution is the optimal solution to the original problem. In this case, the channel of TX-BD is denoted as $\boldsymbol{h}_t$. Then, the L2-norm in (4) is $\|\boldsymbol{H}_r(\boldsymbol{X}_0 - \boldsymbol{X}_1)\boldsymbol{h}_t s\|^2 = \|\boldsymbol{H}_r(\boldsymbol{X}_0 - \boldsymbol{X}_1)\boldsymbol{h}_t\|^2|s|^2$. This readily gives the objective function to be $\|\boldsymbol{H}_r(\boldsymbol{X}_0 - \boldsymbol{X}_1)\boldsymbol{h}_t\|^2$, and the optimal solution is

$$\boldsymbol{X}_0 = -\boldsymbol{X}_1 = \boldsymbol{X}^\star = (1/\|\boldsymbol{h}_t\|_\infty)[\boldsymbol{V}_r]_1\boldsymbol{h}_t^H.$$

B. Diagonal BD Signaling Matrix

By restricting $\boldsymbol{X}_0$ and $\boldsymbol{X}_1$ to be diagonal, the objective function of problem (5) can be rewritten as

$$|||\boldsymbol{H}_r(\boldsymbol{X}_0 - \boldsymbol{X}_1)\boldsymbol{H}_t|||_F^2 = \mathrm{diag}(\boldsymbol{X}_0 - \boldsymbol{X}_1)^H \mathbf{H}^{(2)} \mathrm{diag}(\boldsymbol{X}_0 - \boldsymbol{X}_1),$$

where $\mathbf{H}^{(2)} = \boldsymbol{R}^H\boldsymbol{R}$, and $\boldsymbol{R} = \boldsymbol{H}_t^T \odot \boldsymbol{H}_r$ denotes the Khatri-Rao product of $\boldsymbol{H}_t^T$ and $\boldsymbol{H}_r$. According to the above analysis, the optimal solution is in the direction of the eigenvector associated with the dominant eigenvalue of $\mathbf{H}^{(2)}$. Hence, the optimum diagonal signaling matrix and the corresponding composite channel matrix are given by

$$\begin{aligned}\boldsymbol{X}_0 &= -\boldsymbol{X}_1 = (1/\|[\boldsymbol{V}_R]_1\|_\infty)\mathrm{diag}([\boldsymbol{V}_R]_1) \triangleq \boldsymbol{X}' \\ \boldsymbol{G}(\boldsymbol{X}_i) &= \boldsymbol{H}_d + (-1)^i(\sqrt{\Delta}\sigma_{R,1}/\|[\boldsymbol{V}_R]_1\|_\infty)\mathrm{vec}^{-1}([\boldsymbol{U}_R]_1),\end{aligned}$$

where $[\boldsymbol{V}_R]_1$ is right-singular vector of $\boldsymbol{R}$ associated with the largest singular value $\sigma_{R,1}$. The coefficient $1/\|[\boldsymbol{V}_R]_1\|_\infty$ is multiplied for satisfying the original constraint in Eq. (3).

IV. System Implementation

The *full signaling matrix* requires the signal transfers between BD antenna elements which are represented by the off-diagonal elements of the signaling matrix. In Fig. 2, a realization of the BD modulator capable of transmitting full signaling matrix is shown. The incident signal received on one BD antenna is split into N_b branches. Each branch signal is modulated by the corresponding reflection coefficient. Then, the N_b branches of modulated signals coming from BD antennas are added together to contribute to the signal backscattered

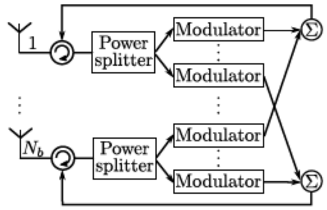

Fig. 2. A design of BD modulator for full signaling matrix.

from BD antennas. On the other hand, for the diagonal signaling matrix, the power splitter and N_b-1 branches of modulator of each BD antenna can be omitted.[2]

A follow-up question is that how can the BD obtain the signaling matrix. We can resort to the more powerful RX, who estimates the BD signaling matrix, and then feeds that to the BD. Even though a receiver is needed at the BD, that for a feedback channel is not power demanding, and the passive receiver presented in [2] can be readily adopted. Nevertheless, the optimum signaling matrix formed by the right- and left-singular vectors of $\boldsymbol{H}_r$ and $\boldsymbol{H}_t$ cannot be extracted directly from their product. Hence, it requires the BD to send specific training sequences for obtaining the signaling matrix.

Within one BD frame, N_b^2+1 preamble sequences are transmitted from the BD, each of which contains K samples. Let $\boldsymbol{X}_{p,\ell} \in \mathbb{C}^{N_b \times N_b}$ denote the ℓ-th BD training sequence, $\ell = 0, \ldots, N_b^2$. The BD first stays silent, i.e., $\boldsymbol{X}_{p,0} = \boldsymbol{0}$, and then, modulator of each branch wakes up to send 1 while other elements are 0. When $\boldsymbol{X} = \boldsymbol{X}_{p,0}$, the direct path channel matrix is estimated as $\hat{\boldsymbol{H}}_d$. When $\boldsymbol{X}_{p,\ell}$ is transmitted, the composite channel, given by $\boldsymbol{G}_\ell \triangleq \boldsymbol{H}_d + \sqrt{\Delta}[\boldsymbol{H}_r]_{\lceil \ell/N_b \rceil}[\boldsymbol{H}_t^T]^T_{(\ell \bmod N_b)}$, is estimated as $\hat{\boldsymbol{G}}_\ell$, where $\lceil \cdot \rceil$ is the ceiling function, and mod is the modulo operator. Then, the backscattered path channel matrix is obtained by $\hat{\boldsymbol{H}}_{b,\ell} = \hat{\boldsymbol{G}}_\ell - \hat{\boldsymbol{H}}_d$, whose vectorization constitutes the ℓ-th column of the matrix $\boldsymbol{Q}$ in Eq. (6), i.e., $[\hat{\boldsymbol{Q}}]_\ell = \mathrm{vec}(\hat{\boldsymbol{H}}_{b,\ell})$. After the training sequences, the optimum full BD signaling matrix $\boldsymbol{X}^\star$ is obtained from the SVD of $\hat{\boldsymbol{Q}}$.

Estimating the diagonal BD signaling matrix $\boldsymbol{X}'$ at the receiver needs only N_b+1 training sequences, within which the BD first stays silent, and then, each BD antenna wakes up and sends 1. Compared with $\boldsymbol{X}'$, the amount of circuitry components and the number of training sequences for transmitting $\boldsymbol{X}^\star$ quadratically grows with N_b.

The channel estimation can be done by using, for example, the maximum likelihood (ML) estimator which requires the information of ambient signal. It can be realized by attaching a standard ambient signal receiver to the AmBC receiver. This method is feasible when all the ambient sources belong to the same type, such as multiple DVB-T base stations. However, it is challenging for the AmBC receiver to acquire the information of different types of ambient sources.

To lift the constraint on knowing the ambient signal, one can configure the BD with an RF chain. The BD then estimates the signal direction associated with the strongest signal power towards the TX. The beamformer toward the RX can be acquired from the RX using channel reciprocity. Such an implementation can be realized using the beam-steerable transponder [8] and energy detector at the BD.

Finally, lowering the resolution of each modulator can reduce the manufacturing cost and power consumption of BDs because it decreases the required bits for the RX to feedback the optimum $\boldsymbol{X}$. Since the optimum $\boldsymbol{X}$ is a beamforming matrix, a feasible discretized set can be the set of quantized beamforming angles and the signaling matrices are formed by the steering vectors. Furthermore, the modulator resolution in turn decides the performance of the signaling matrix.

V. Numerical Results

We evaluate the performance of the derived signaling matrices in terms of the BER of the AmBC system. We utilize a receiver extended from an available optimum AmBC receiver derived for the Gaussian ambient signal [6], [17].

As shown in Fig. 1(b), a practical scenario where three TXs ($N_t = 3$) are dis-located in a hexagonal cell structure is considered. The distance is normalized with respect to wavelength to make the simulation results frequency-agnostic. The three TXs, whose coverage radius is 1000λ, are placed in a two-dimensional Cartesian coordinate system, whose origin is the $\lceil N_r/2 \rceil$-th RX antenna and the y-axis is aligned with the linear RX array. The RX is 900λ away from the closest TX. The number of RX antenna is set to be $N_r = 8$, and the BD modulator circuit loss is $\alpha = 0.6$. The TXs transmit i.i.d. signal with the same averaged transmit power P_s which is calculated from a given SNR of the direct path signal γ. The BD data is drawn from the equiprobable binary phase shift keying modulation.

In Fig. 3, a square area with 20λ length of sides is considered. The SNR of the direct path $\gamma = 27$ dB. BER performance of single-antenna TX and single-antenna BD is selected as the benchmark. Fig. 3(a) to Fig. 3(c) show the BER performance gain of using single or multiple antennas at the BD and of using different BD signaling matrix compared to the benchmark. As can be seen, using a single BD antenna cannot benefit from multiple ambient sources. Using the identity signaling matrix brings a significant performance gain when the BD is extremely close to the RX, i.e., less than 3λ, which decays fast as the distance between the RX and the BD increases. Using the optimum signaling matrix robustly improves the BER performance in the selected area, i.e., giving roughly a 15 dB gain. It is to be noted that the derived signaling matrix provides the optimum solution of the relaxed problem, as shown in Fig. 3(d) that $\boldsymbol{X}^\star$ always yields a higher averaged backscatter signal power. Hence, using multiple BD antennas effectively utilizes the multiple ambient sources. The identity signaling matrix provides a better BER performance under certain channel condition while the derived BD signaling matrix largely improves the coverage of AmBC communication.

Next, we evaluate the proposed estimation scheme for the optimum signaling matrices. The coordinates of the $\lceil N_b/2 \rceil$-th BD antenna is $(-3\sqrt{2}\lambda, -3\sqrt{2}\lambda)$. Such a deployment results in the power difference between two paths to be $\Delta \approx -39$ dB. The impact of the length of training sequence K on the estimation method when $\gamma = 27$ dB and $N_b = 4$ is shown in Fig. 4(a). The estimation for $\boldsymbol{X} = \boldsymbol{X}'$ converges slower than that for $\boldsymbol{X} = \boldsymbol{X}^\star$ as K increases. For two signaling matrices, the BER performance improves marginally after $K \geq 100$. Therefore, the introduced estimation process is effective and $K = 100$ can provide an acceptable performance.

In Fig. 4(b), the discretized signaling matrices are evaluated in two cases: $\boldsymbol{X}$ is formed by steering vectors and every modulator of $\boldsymbol{X}$ has one bit, i.e., $[X]_{i,j} \in \{-1, 1\}$. For the former set, the optional angles are $\phi, \theta \in \{0, \pi/4, \pi/2, 3\pi/4\}$ such that the diagonal $\boldsymbol{X} = \mathrm{diag}(\boldsymbol{\alpha}(\theta))$ and the full $\boldsymbol{X} =$

[2]We assume that the BD has harvested enough energy for receiving the signaling matrix and modulating each branch.

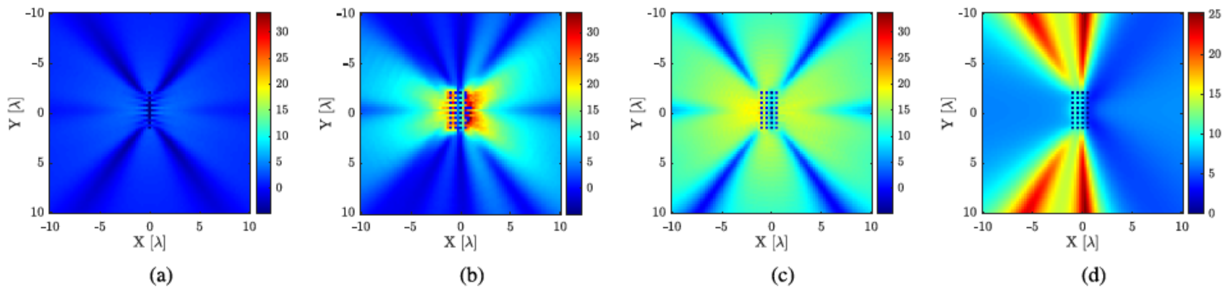

Fig. 3. In (a)-(c), the BER performance gain of using multiple antennas at the BD and/or difference BD signaling matrix under multi-antenna TX compared to using single antenna at both the BD and the TX. The BER ratio in dB of (a) $N_t = 3, N_b = 1$, (b) $N_t = 3, N_b = 4, \boldsymbol{X} = \boldsymbol{I}$, and (c) $N_t = 3, N_b = 4, \boldsymbol{X} = \boldsymbol{X}^\star$ to $N_t = N_b = 1$. In (d), the difference of averaged received backscatter signal power in dB between $\boldsymbol{X} = \boldsymbol{I}$ and $\boldsymbol{X} = \boldsymbol{X}^\star$.

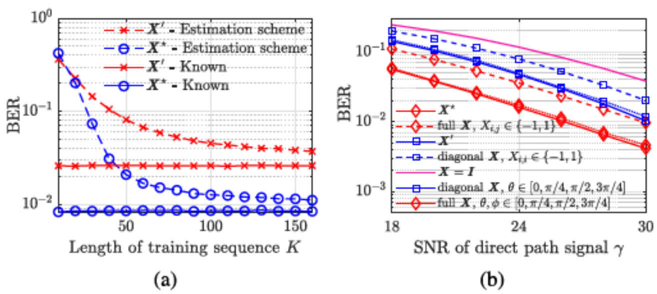

Fig. 4. In (a), BER performance as a function of K for estimating the optimum full and diagonal signaling matrices. In (b), BER comparison between the optimum $\boldsymbol{X}$ and discretized signaling matrices.

$\boldsymbol{\alpha}(\theta)\boldsymbol{\alpha}(\phi)^H$, where the k-th element of the steering vector is $[\boldsymbol{\alpha}(\theta)]_k = \exp(-j\pi \cos\theta(k-1))$. The cardinalities of the two cases are 16 and 2^{16}, respectively, while the former requires a higher resolution. As can be seen, with properly quantized beamformers, the BD signaling matrix outperforms the 1-bit modulator and approaches the continuous resolution.

VI. Conclusion

We study the BD signaling matrix to improve the AmBC system performance when multiple ambient sources are illuminating the BD. The optimum full and diagonal signaling matrices for the multi-antenna backscatter device are derived, which combine the ambient signal and steer the backscatter signal toward the receiver to improve the backscatter signal power. Compared with the full signaling matrix, the diagonal BD signaling matrix has a performance loss, but saves the training time and circuit components. The simulation results validate the proposed estimation method for the BD signaling matrices and demonstrate that they can be used to robustly enlarge the communication range or improve the datarate of the backscatter device.

References

[1] R. Duan, X. Wang, H. Yigitler, M. U. Sheikh, R. Jantti, and Z. Han, "Ambient backscatter communications for future ultra-low-power machine type communications: Challenges, solutions, opportunities, and future research trends," *IEEE Commun. Mag.*, vol. 58, no. 2, pp. 42–47, Feb. 2020.

[2] A. N. Parks, A. Liu, S. Gollakota, and J. R. Smith, "Turbocharging ambient backscatter communication," in *Proc. ACM SIGCOMM*, Chicago, IL, USA, 2014, pp. 619–630.

[3] M. A. ElMossallamy, M. Pan, R. Jäntti, K. G. Seddik, G. Y. Li, and Z. Han, "Noncoherent backscatter communications over ambient OFDM signals," *IEEE Trans. Commun.*, vol. 67, no. 5, pp. 3597–3611, May 2019.

[4] G. Yang, Y.-C. Liang, R. Zhang, and Y. Pei, "Modulation in the air: Backscatter communication over ambient OFDM carrier," *IEEE Trans. Commun.*, vol. 66, no. 3, pp. 1219–1233, Mar. 2018.

[5] X. Wang, H. Yiğitler, R. Duan, E. Y. Menta, and R. Jäntti, "Coherent multiantenna receiver for BPSK-modulated ambient backscatter tags," *IEEE Internet Things J.*, vol. 9, no. 2, pp. 1197–1211, Jan. 2022.

[6] H. Yiğitler, X. Wang, and R. Jäntti, "Optimum multi-antenna ambient backscatter receiver for binary-modulated tag signals," *IEEE Trans. Wireless Commun.*, early access, Aug. 19, 2022, doi: 10.1109/TWC.2022.3198514.

[7] C. Yang, J. Gummeson, and A. Sample, "Riding the airways: Ultra-Wideband ambient backscatter via commercial broadcast systems," in *Proc. IEEE Infocom*, May 2017, pp. 1–9.

[8] T. A. Siddiqui, J. Holopainen, and V. Viikari, "Beam-steerable transponder based on antenna array and phased modulators," *IEEE Antennas Wireless Propag. Lett.*, vol. 20, pp. 356–360, 2021.

[9] C. Chen, G. Wang, H. Guan, Y.-C. Liang, and C. Tellambura, "Transceiver design and signal detection in backscatter communication systems with multiple-antenna tags," *IEEE Trans. Wireless Commun.*, vol. 19, no. 5, pp. 3273–3288, May 2020.

[10] A. H. Raghavendra, A. K. Kowshik, S. Gurugopinath, S. Muhaidat, and C. Tellambura, "Generalized space shift keying for ambient backscatter communication," *IEEE Trans. Commun.*, vol. 70, no. 8, pp. 5018–5029, Aug. 2022.

[11] W. Liu, S. Shen, D. H. K. Tsang, and R. Murch, "Enhancing ambient backscatter communication utilizing coherent and non-coherent space-time codes," *IEEE Trans. Wireless Commun.*, vol. 20, no. 10, pp. 6884–6897, Oct. 2021.

[12] J. Kimionis, A. Georgiadis, S. N. Daskalakis, and M. M. Tentzeris, "A printed millimetre-wave modulator and antenna array for backscatter communications at gigabit data rates," *Nat. Electron.*, vol. 4, pp. 439–446, Jun. 2021.

[13] J. D. Griffin and G. D. Durgin, "Gains for RF tags using multiple antennas," *IEEE Trans. Antennas Propag.*, vol. 56, no. 2, pp. 563–570, Feb. 2008.

[14] J. M. Wozencraft and I. M. Jacobs, *Principles of Communication Engineering*. New York, NY, USA: Wiley, 1965.

[15] D. Tse and P. Viswanath, *Fundamentals of Wireless Communication*. Cambridge, U.K.: Cambridge Univ. Press, 2005.

[16] R. A. Horn and C. R. Johnson, *Topics in Matrix Analysis*. Cambridge, U.K.: Cambridge Univ. Press, 1991.

[17] H. Guo, Q. Zhang, S. Xiao, and Y.-C. Liang, "Exploiting multiple antennas for cognitive ambient backscatter communication," *IEEE Internet Things J.*, vol. 6, no. 1, pp. 765–775, Feb. 2019.